Outliers, extreme events, and multiscaling

3 authors, including:

Victor S. L'vov
Weizmann Institute of Science
319 PUBLICATIONS   **6,281** CITATIONS

SEE PROFILE

Anna Pomyalov
Weizmann Institute of Science
79 PUBLICATIONS   **984** CITATIONS

SEE PROFILE

Some of the authors of this publication are also working on these related projects:

Project   Adsorption of metal atoms of reconstructed Si surfaces View project

Project   Superfluid counterflow turbulence in a channel View project

Outliers, extreme events, and multiscaling

Victor S. L'vov, Anna Pomyalov, and Itamar Procaccia

Department of Chemical Physics, The Weizmann Institute of Science, Rehovot 76100, Israel

(Received 26 September 2000; published 20 April 2001)

Extreme events have an important role which is sometimes catastrophic in a variety of natural phenomena, including climate, earthquakes, and turbulence, as well as in manmade environments such as financial markets. Statistical analysis and predictions in such systems are complicated by the fact that on the one hand extreme events may appear as ''outliers'' whose statistical properties do not seem to conform with the bulk of the data, and on the other hand they dominate the tails of the probability distributions and the scaling of high moments, leading to ''abnormal'' or ''multiscaling.'' We employ a shell model of turbulence to show that it is very useful to examine in detail the dynamics of onset and demise of extreme events. Doing so may reveal dynamical scaling properties of the extreme events that are characteristic to them, and not shared by the bulk of the fluctuations. As the extreme events dominate the tails of the distribution functions, knowledge of their dynamical scaling properties can be turned into a prediction of the functional form of the tails. We show that from the analysis of relatively short-time horizons (in which the extreme events appear as outliers) we can predict the tails of the probability distribution functions, in agreement with data collected in very much longer time horizons. The conclusion is that events that may appear unpredictable on relatively short time horizons are actually a consistent part of a multiscaling statistics on longer time horizons.

I. INTRODUCTION

There is an obvious and widespread interest in predicting extreme events in a variety of contexts. Particularly well-known examples are the insurance risks related to large tropical storms, human and property risks in the context of large earthquakes, financial risks caused by large movements of the markets, and dangers to passenger planes due to extremely intermittent turbulent air velocities. Obviously, any improvement in the predictability of any of these extreme events is highly desirable for a number of reasons. Accordingly, there exists a large body of work focusing on the statistics of such events, small, intermediate, and large, with the aim of studying the ensuing probability distribution functions (PDF). If one can model properly the PDF, one can, in principle, predict at least the frequency of extreme events. Yet, there is one fundamental question that arises that needs to be confronted first: are the extreme events sharing the same statistical properties as the small and intermediate events, or are they ''outliers?'' If the latter is true, then no analysis of the core of the PDF, clever as it may be, could yield a proper answer to the desire to predict the probability of extreme events.

Indeed, in a number of contexts it had been proposed recently that extreme events are ''outliers'' [1]. For example, in financial markets the largest draw downs appear to exhibit properties that differ from the bulk of the fluctuations [2]. In general one would refer to ''outliers'' when the rate of occurrence of small and intermediate events lies on a PDF with some given properties, while the extreme events appear to exhibit statistical properties that differ from the bulk in a significant way. The aim of this paper is to present a detailed analysis of the fluctuations in a turbulent dynamical system that shows that such a point of view can be substantiated. Clearly, this type of consideration must be conducted with great care. The danger is that on small time horizons the

largest events appear so rarely, once or twice, that their rate of occurrence is not statistically significant, and no conclusion about their relation to the statistics of small and intermediate events is possible. Nevertheless, we offer in this paper a positive outlook. We will show that in the context of the bulk of this paper, which is the analysis of a shell model of turbulence, one can analyze *within the short time horizon* the dynamics of the extreme events. This analysis reveals their special dynamical scaling properties, allowing us to make interesting predictions about the tails of the distribution functions even before the full statistics is available. These predictions can be checked in our case by considering much longer time horizons. The conclusion for the extreme events community is that it may very well pay to look very carefully at the detailed dynamics of the extreme events if one wants to claim anything about their probability of occurrence.

The model that we treat in detail in this paper is a so-called ''shell'' model of turbulence. Shell models of turbulence [3–8] are simplified caricatures of the equations of fluid mechanics in wave-vector representation; typically they exhibit anomalous scaling even though their nonlinear interactions are local in wave-number space. The wave numbers are represented as shells, which are chosen as a geometric progression

$$k_n = k_0 \lambda^n, \tag{1}$$

where λ is the ''shell spacing.'' There are N degrees of freedom where N is the number of shells. The model specifies the dynamics of the ''velocity'' u_n which is considered a complex number, $n = 1, \ldots, N$. Their main advantage is that they can be studied via fast and accurate numerical simulations, in which the values of the scaling exponents can be determined very precisely. We employ our own homemade shell model which had been christened the Sabra model [8].

It exhibits similar anomalies of the scaling exponents to those found in the previously popular model by Gledzer [3] and Yamada and Ohkitani [4] (the GOY model), but with much simpler correlation properties, and much better scaling behavior in the inertial range. The equations of motion for the Sabra model read

$$\frac{du_n}{dt} = i(ak_{n+1}u_{n+2}u_{n+1}^* + bk_nu_{n+1}u_{n-1}^* - ck_{n-1}u_{n-1}u_{n-2})$$
$$- \nu k_n^2 u_n + f_n, \qquad (2)$$

where the asterisk stands for complex conjugation, f_n is a forcing term which is restricted to the first shells, and ν is the "viscosity." In this paper we restrict the forcing to the first and and second shells only ($n=1,2$). The coefficients a, b, and c are chosen such that

$$a+b+c=0. \qquad (3)$$

This sum rule guarantees the conservation of the "energy"

$$E=\sum_n |u_n|^2, \qquad (4)$$

in the inviscid ($\nu=0$) limit.

The main attraction of this model is that it displays multiscaling in the sense that moments of the velocity depend on k_n as power laws with nontrivial exponents,

$$S_p(k_n) \equiv \langle |u_n|^p \rangle \propto k_n^{-\zeta_p} \propto \lambda^{-n\zeta_p}, \qquad (5)$$

where the scaling exponents ζ_p exhibit nonlinear dependence on p. We expect such scaling laws to appear in the "inertial range" with shell index n larger than the largest shell index that is effected by the forcing, denoted as n_L, and smaller than the shell indices affected by the viscosity, the smallest of which will be denoted as n_d. The scaling exponents were determined with high numerical accuracy better than 0.02 in Ref. [8].

To introduce the issue behind the title of this paper, we present in Fig. 1 a typical time series for u_{11}. The parameters of the model are detailed in the figure legend. One can see the typical appearance of rare events with amplitude that exceeds the mean by a factor of 6–8. To pose the question in its clearest way we display in Fig. 2 a distribution function which is the normalized rate of occurrence (i.e., the number of times) that a given amplitude has been observed in the time window of 10^7 time steps. This apparent relative frequency of events is very similar to findings in real data, see for example Fig. 1 of Ref. [2], which deals with draw downs in the Dow Jones Average. Similarly to the analysis there, we can pass an approximate straight line through the points representing small and intermediate events. Such an exponential law would mean that the events of $|u_{11}|^2$ with amplitudes larger than, say, $4\langle |u_{11}|^2 \rangle$ are clear outliers. Their probability is so low that they should not have appeared in the short time horizon at all. We could conclude, like in the
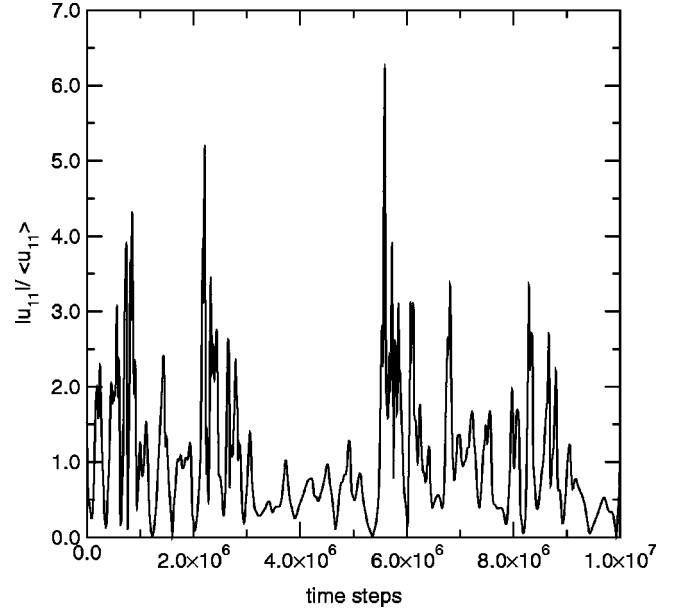

FIG. 1. Time series for the normalized velocity of the 11th shell. Parameters of the numerics: $a=1$, $b=c=-0.5$, $\lambda=2$, $N=28$, $k_0 = \frac{1}{64}$; time correlated random forcing on the first two shells with characteristic amplitude 0.005 $(1+i)$. Decorrelation time is chosen about turnover time of the first shell.

analysis of Ref. [2], that the extreme events cannot be dealt with the same distribution function as the small and intermediate events.

On the other hand, it is very possible that the low rate of occurrence of the extreme events in Fig. 2 means simply that they are statistically irrelevant and that no conclusion can be drawn. How do we overcome this difficulty? The purpose of this paper is to show that indeed the extreme events may have dynamical scaling properties that are all their own, and that they affect crucially the tails of the distributions func-
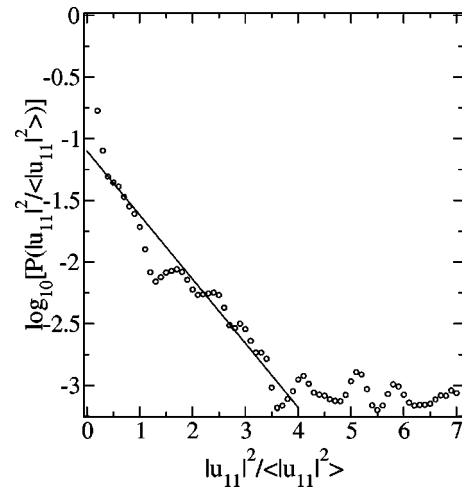

FIG. 2. Apparent probability distribution function for the 11th shell. Averaging over 10^7 time steps which is about 250 decorrelation times for this shell. The data contain additional, extremely sparse events of amplitude larger than 7, occurring once each; these were left out in this plot.

tions, making them very broad indeed. The main new point is that a detailed analysis of the extreme events *in the short time horizon* suffices to make lots of predictions about the tails of the PDF's, predictions that in our case can be easily confirmed by considering much longer time horizons.

In explaining our ideas we will try to distinguish aspects which are general, and that in our view may have applications to other systems with extreme events, and aspects which are particular to the example of the shell model of turbulence. Thus we start in Sec. II with an analysis of the temporal shape of the extreme events. We believe that this analysis is very general, leading to an important relation between the amplitude of the event and its time scale (the time elapsing from rise up to demise). In Sec. III we employ the dynamical scaling form of the extreme events to present a theory of the tails of the distribution functions. We can relate the tails of PDF's belonging to different scales. In Sec. IV we discuss numerical studies of the PDF's, distinguishing the core and the tails. In Sec. V the main numerical findings are rationalized theoretically on the basis of universal ''pulse'' solutions of the dynamics of the Sabra model. Section VI contains the bottom line: we make use of the scaling relations to *predict* the tails of PDF's from data collected within short time horizons. Direct measurements of these tails give nonsense unless the time horizons are increased a hundred-fold. Yet with the help of the theoretical forms we can offer predicted tails that agree very well with the data collected with much longer time horizons.

II. DETAILED DYNAMICS AND SCALING OF THE EXTREME EVENTS

In turbulence in general and in our shell model in particular the energy that is injected by the forcing at the largest scales ($n=1$ and 2) is transferred on the average to smaller scales. It is advantageous to analyze the extreme events of a given scale (or given shell n) and also to follow the cascade of extreme events from scale to scale. We first consider a given shell.

A. Temporal dependence of extreme events of a given scale

We focus here on the detailed dynamics of the largest events of a given scale. We considered, for example, the time series of the 20th shell ($n=20$) and isolated the five largest events (in terms of their amplitude) as they occurred in a time window of 10^7 time steps. In the first step of analysis we normalized these five events by the amplitude at their maximum. Next we plotted these normalized events as a function of time, subtracting the time at which they have reached their maximum value. The result of this replotting is shown in Fig. 3. Obviously a similar replotting can be done for any time series, and by itself is contentless.

The next step of analysis will reveal something interesting. Building on the normalized events of Fig. 3 we attempt to rescale the time axis for each event in order to collapse the data together. Of course, each event calls for a different rescaling factor, which we denote (in frequency units) as f_r. The fact that such rescaling factors exist, and that they lead
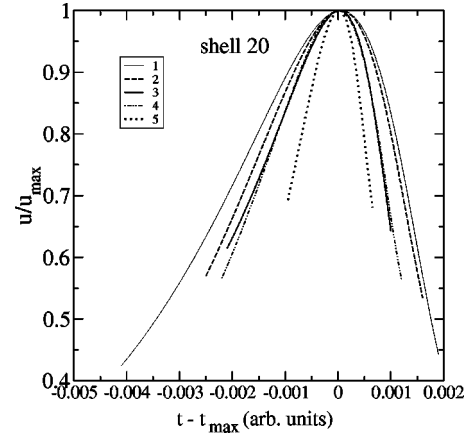

FIG. 3. Collapse (of positions and amplitudes) for five intensive peaks belonging to the 20th shell. The values of u_{max} for the peaks numbered from 1 to 5 are 4.65, 4.77, 6.71, 7.40, and 10.5, respectively, in units of the rms velocity in this shell. The narrowest peak is thus the tallest.

to data collapse as shown in Fig. 4, is not a trivial fact that may or may not exist in different cases. But we will show that if such a rescaling is found, it can serve as a starting point for very useful considerations.

The third step of the present analysis is a search of meaning to the rescaling factors f_r. We hope that f_r has a simple relation to the amplitude of the extreme events. To test this we can plot the individual values of f_r found in Fig. 4 as a function of the amplitude at the peak. The resulting plot is shown as Fig. 5. In passing the straight line through the data points we included the point (0,0) in the analysis, as we search for a simple scaling form

$$f_r \propto u_{max}^x, \tag{6}$$

with x a scaling exponent. We conclude that in this case we have a satisfactory scaling law with $x=1$.

The meaning of this scaling law is quite apparent in the present case. Looking back at the equation of motion we
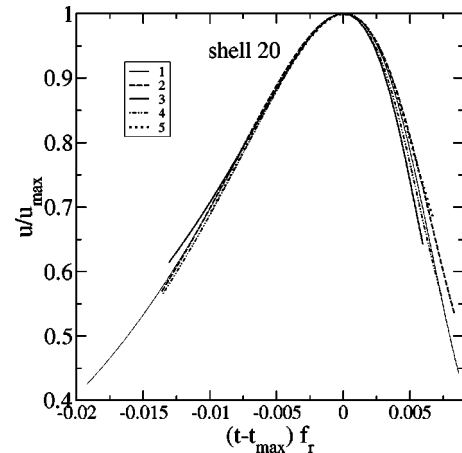

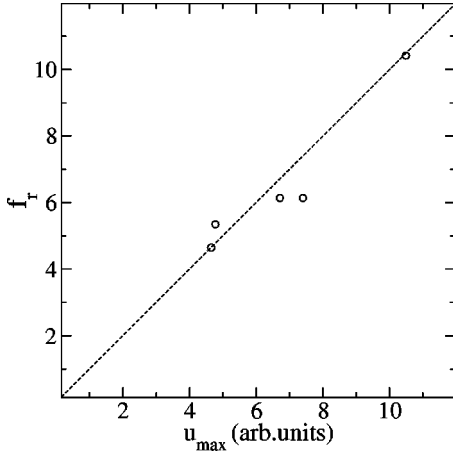FIG. 4. Full collapse (of the position, amplitude, and width) of the same as in Fig. 3 peaks.

FIG. 5. Width normalization vs amplitude for the five collapsed peaks of Fig. 4. The ordering of the points is 1 to 5 from left to right.

realize that from the point of view of power counting (not to be confused with actual dynamics) it can be written as

$$\frac{du}{dt} \propto u^{1+x} \qquad (7)$$

with $x=1$. It is thus acceptable that a rescaling of $1/t$ by u_{max} should collapse all the extreme events as shown above. If the equation of motion were cubic in u we could expect $x=2$, etc. Obviously, the rescaling analysis in this case revealed the type of dynamics underlying the process. Whether this can be done effectively in other cases where extreme events are crucial is an open question for future research.

B. Transfer of extreme events between different scales

To gain further understanding of the extreme events we focus now on the transfer from scale to scale. Consider, for example, a particular large amplitude event in the shell $n = 15$, and its future fate as time proceeds. This is shown in Fig. 6. The event reached its highest amplitude at shell 15 around $t=2.625$. At a slightly later time it appeared as a large event in shell 16, and with a shorter delay at shell 17 where it started to split into a doublet. At even shorter delays this event emerges as a triplet and a multiplet at shells 18, 19, and 20, respectively.

A very important characteristic of the dynamics of large events can be obtained from finding how to relate the maximal amplitudes of the first peak in the different shells. As was done above, we first replot all the first peaks as a function of time minus the time t_n of their maximal amplitude $u_{n,max}$. We then glue all the maxima together by rescaling the peak amplitudes relative to the peak of a chosen shell. We denote by $K_{am}(n,m)$ the relative amplitude of the peak in the nth shell to the mth shell. Choosing in our example $m=20$ we then seek a single exponent y such that

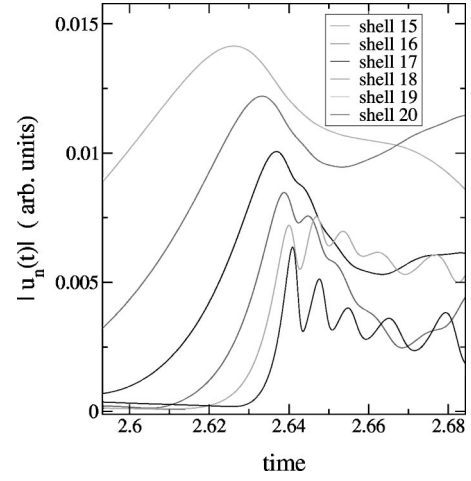$$K_{am}(n,20) \equiv u_{n,max}/u_{20,max} = \lambda^{(20-n)y}, \qquad (8)$$

FIG. 6. ''Evolution'' of a peak from the 15th to the 20th shell. The amplitudes are all in the same (arbitrary) units. One sees a progressive shift of the maximum to the right and a decrease in the amplitude, accompanied by narrowing and splitting. Nevertheless the form of the central part of the peak remains self-similar as exemplified in Figs. 7 and 8.

where λ is the shell spacing defined by Eq. (1). The value of y is obtained by plotting $g_{am}(n)$ vs $(20-n)$ where

$$g_{am}(n) \equiv \ln[K_{am}(n,20)]/\ln \lambda = y(20-n). \qquad (9)$$

The best fit is obtained with $y=0.24\pm0.01$, see Fig. 9. The peaks which are now glued at their maxima as shown in Fig. 7 still have a very different time width.

Next, as before, we want to collapse all these curves by rescaling the time axis according to $(t-t_n) \to (t -t_n)/K_w(n,20)$. Expecting the scaling law $K_w(n,20) = \lambda^{z(20-n)}$ it is natural to consider

$$g_w(n) \equiv \ln[K_w(n,20)]/\ln \lambda = z(20-n). \qquad (10)$$

The exponent $z=0.75\pm0.02$ is found by computing ''the best'' linear fit of $g_w(n)$ vs $(20-n)$, see Fig. 9. The quality
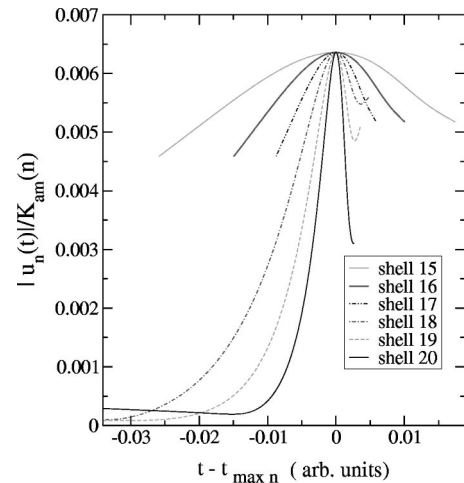

FIG. 7. Collapse of the peak amplitudes for 15–20 shells. Initial peaks are shown in Fig. 6.
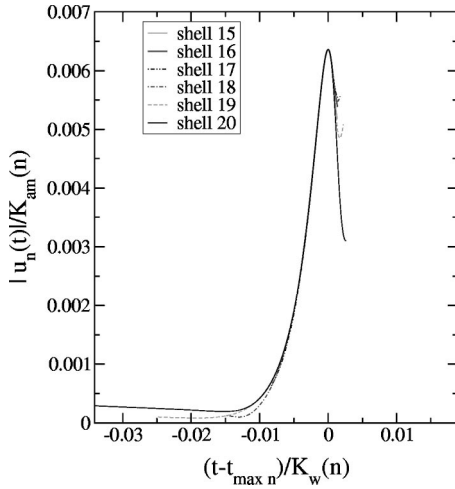
FIG. 8. Full self-similar collapse of the peaks for 15–20 shells.

of the resulting data collapse can be seen in Fig. 8. Note that within the error bars $z+y=1$. This sum rule will be rationalized theoretically in Sec. V.

The bottom line of this analysis can be summarized in a dynamical scaling form for the extreme events

$$u_n(t) \approx v\lambda^{-yn} f((t-t_n)vk_0\lambda^{zn}). \tag{11}$$

Here v is a characteristic velocity amplitude associated with the cascade of a particular large event which starts at small n and reaches eventually large values of n. As such v is not universal. We stress that the scaling form was derived on the basis of a time series in the short time horizon, i.e., the the same one that gave rise to the apparent PDF shown in Fig. 2. We will see that these findings suffice to make rather strong predictions about the expected form of the *converged* PDF. A theoretical understanding of the origin of the scaling form (11) will be presented in Sec. V.
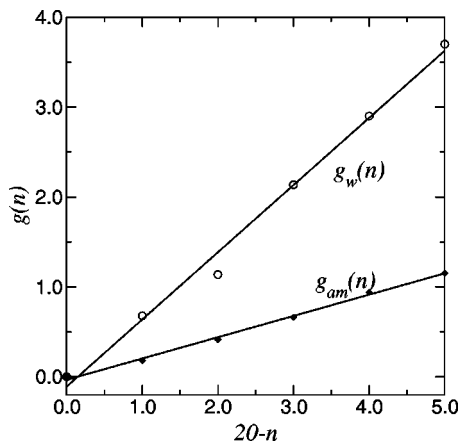

FIG. 9. Fits of the rescaling factors $g_w(n)$ and $g_{am}(n)$ for the peaks in the shells 15–20 shown in Figs. 6, 7, and 8. Note that in comparing *different* shells the rescaling of the frequency increases when the peak decreases in amplitude. This is opposite to the rescaling of peaks *within* a given shell.
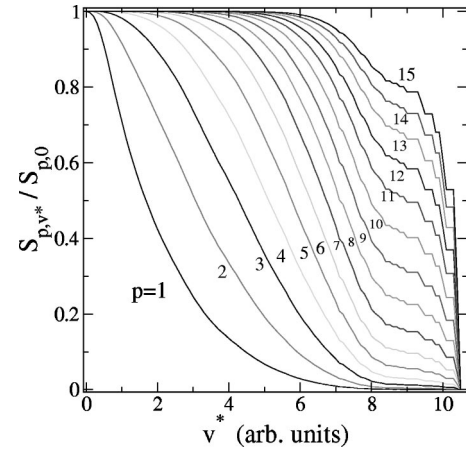

FIG. 10. Normalized contributions to the structure functions of orders $p=1,2,\ldots,15$ for the 20th shell from the part of the velocity realization with $v>v_*$.

III. IMPLICATIONS FOR THE TAILS OF THE PROBABILITY DISTRIBUTION FUNCTIONS

A. Asymptotic scaling exponents

Having a scaling form for the large events means a great deal for the structure functions $S_p(k_n)$ [cf. Eq. (5)] for high values of p. In fact for high p the structure functions are dominated by the large events. To demonstrate this we show in Fig. 10 the relative contribution to $S_p(k_{20})$ that arises from velocity amplitudes that exceed a threshold v_*. In this plot S_{p,v_*} is the structure function Eq. (5) where only events with $u_{20} \geqslant v_*$ are considered, whereas $S_{p,0}$ contains all the data. Obviously the higher p is, the higher the contribution is of large events. For any time window there exists the largest event, and when v_* exceeds its value, S_{p,v_*} necessarily vanishes.

If we accept the scaling form (11) we can use it to predict the scaling exponent ζ_p for high values of p. By definitions

$$S_p(k_n) = \lim_{T\to\infty} \frac{1}{2T}\int_{-T}^{T}|u_n|^p dt \propto k_n^{-\zeta_p} \propto \lambda^{-n\zeta_n}. \tag{12}$$

For p large enough the structure functions are dominated by the well separated events. Instead of the integral in the interval $[-T,T]$ we can sum up the inegrals over the separated peaks. Substituting for each peak the form (11) and noting that the number of peaks is proportional to T, we can extend the integration interval to $[-\infty,\infty]$ and write

$$S_p(k_n) \propto \lambda^{-ynp}\int_{-\infty}^{\infty} f^p(\lambda^{zn}tvk_0)dt \propto \lambda^{-n(yp+z)}\int_{-\infty}^{\infty} f^p(\tau)d\tau. \tag{13}$$

Comparing the exponents of λ here and in the previous equation we find the scaling exponents

$$\zeta_p = yp + z. \tag{14}$$

Of course this prediction is valid only for high values of p for which the contributions of the isolated peaks are domninant.

B. Tails of the probability distribution function

We turn now to the prediction of the tails of the PDF's, assuming that these tails are dominated by well-separated peaks with self-similar evolution (11). We will see below [and cf. Eq. (19)], that the tails of the predicted PDF are very sensitive to the *exponents* in Eq. (11), but rather insensitive to the precise form of the universal function $f(x)$ in Eq. (13). Assume then for simplicity that $f(x)=1$ for $|x| \leqslant \frac{1}{2}$ and $f(x)=0$ for $|x| > \frac{1}{2}$. There is the free parameter v in Eq. (11); for the chaotic realizations $u_n(t)$ we consider it as a random parameter. Define then the variable V^2 according to

$$V^2 \equiv v^2/v_0^2, \quad v_0^2 = \sum_{n=1}^{\infty} \langle u_n^2 \rangle. \quad (15)$$

Consider now a run with a total time horizon $T \equiv 1/(k_0 v_0)$. Denote as $W(V^2)dV^2$ the number of peaks measured in this run in which the value of V^2 fell in the window $[V^2,(V^2+dV^2)]$.

Next denote normalized amplitudes [the value of the signal at times $t = t_n$ in Eq. (11)]

$$U_n^2 \equiv \frac{u_n^2}{\langle u_n^2 \rangle} = \frac{V^2}{C\lambda^{\alpha n}}, \quad \alpha \equiv 2y - \zeta_2, \quad (16)$$

where C is a dimensionless constant. We are interested in the PDF $P_n(U_n^2)$, where $P_n(U_n^2)dU_n^2$ is the probability to sample a normalized amplitude in the nth shell between U_n^2 and $U_n^2 + dU_n^2$. By definition, the number of observations of such amplitudes in the time horizon T is dN_n

$$dN_n = P_n(U_n^2)dU_n^2 \frac{T}{\tau_0}, \quad (17)$$

where τ_0 is the length of the sampling intervals. On the other hand, since the lifetime of a peak with a given value of V^2 belonging to the nth shell is $1/v k_0 \lambda^{zn}$, we can also estimate the number of observations dN_n as

$$dN_n = \frac{W(V^2)}{\tau_0 v k_0 \lambda^{nz}} dV^2. \quad (18)$$

Equating Eqs. (17) and (18) and rearranging, one gets

$$P_n(U_n^2) = CW(V^2)\lambda^{n(\alpha-z)}/V. \quad (19)$$

This relation is obtained under the assumption that the number of peaks is not increasing in the cascade process. In fact we saw that the number of the peaks is increasing with the shell number n, presumably in a scale-invariant manner as λ to some positive exponent β. We can account for this effect by replacing in Eq. (19) W by $\lambda^\beta W$. After that

$$P_n(U_n^2) = CW(V^2)\lambda^{n(\alpha+\beta-z)}/V, \quad (20)$$

where V^2 and U_n^2 are defined by Eqs. (15) and (16). Equation (20) means that a collapse of the tails of the PDF's for different shells may be achieved by rescaling the x axis $U_n^2 \to V^2$ according to Eq. (16) and rescaling of the PDF's (y axis) by $\lambda^{n(\alpha+\beta-z)}$.

Equation (20) for the tail of the PDF's allows one to find the high-order structure functions (which are dominated by the tails of the PDF's) and their scaling exponents ζ_p

$$S_p(k_n) = \int_0^\infty u_n^p P_n(U_n^2)d U_n^2 = C_p v_0^p \lambda^{n(\beta-z-yp)}, \quad (21)$$

$$C_p = \int_0^\infty V^{p-1} W(V^2)V^2. \quad (22)$$

Comparing again the exponents of λ here and in Eq. (12) gives the prediction for the high-order scaling exponents

$$\zeta_p = yp + z - \beta, \quad (23)$$

which coincides with Eq. (14) at $\beta=0$. One sees that the effect of peak splitting (which was described by the positive exponent β) increases the deviation of the scaling exponents from its Kolmogorov 1941 (K41) value $\zeta_p = p/3$.

IV. NUMERICAL STUDIES OF THE PDF: CORE AND TAIL

It is well known that PDF's in multiscaling systems are not scale invariant. Nevertheless we need to examine the possibility that the cores of the PDF's can be collapsed using a rescaling law that is charateristic to them, while the tails may be collapsed using another rescaling law (with different scaling exponents). This possibility is related to the fact that the structure functions $S_p(k_n)$ have scaling exponents in the vicinity of the K41 values $[\zeta_{\text{K41}}(p) = p/3]$ for p small enough (say, $p \leqslant 6$). For large value of p (say, $p > 12$) the p dependence of ζ_p has a different slope, cf. Eq. (23). These differences result from the core of PDF's originating from the bulk of the fluctuations while the tail of PDF's results from the well-separated high amplitude peaks. Accordingly the functional form of the core and the tail of the PDF's are different. This is demonstrated in Fig. 11 (upper panel) where the PDF's for the 11th, 15th, and 18th shells are displayed. One sees that the cores (say, $U_n^2 \leqslant 20$) are practically collapsed while the tails are widely separated. Needless to say, the collapse is due to our choice of display as a function of U_n^2: for K41 PDF's such a display would result in a complete collapse, core as well as tail. We stress, though, that if one expanded the scale one could observe that the collapse of the core is not precise: the scaling exponents even for $p=2$ and $p=4$ are *not* $\frac{2}{3}$ and $\frac{4}{3}$, respectively. The anomaly of these exponents is, however, sufficiently small to allow an approximate collapse of the cores.

Our aim here is to test the predictions regarding the tails of the PDF's. We note that PDF's that originate from data tend to have rather noisy tails. This poses difficulties in assessing the accuracy of the collapse of the tails. Therefore we opt to first fit the PDF's with some appropriate functional
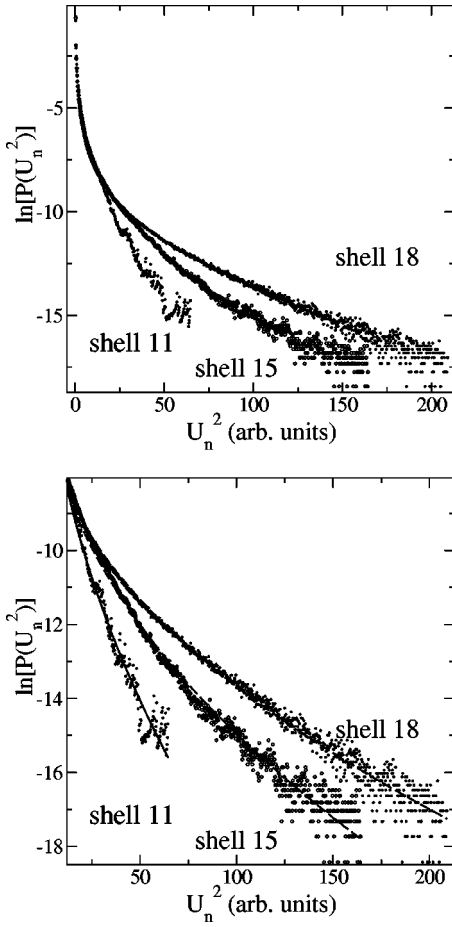
FIG. 11. Upper panel: PDF's of the 11th, 15th, and 18th shells (averaged over 10^9 time steps). Lower panel: Tails of PDF's (with the cores left out) fitted by functions of the form $\ln[P_n(U_n^2)]=a_n+b_nU_n$ (continuous lines).

form and then to collapse the fit functions. As a natural fit function we choose $\ln[P_n(U_n^2)]=a_n+b_nU_n^{2c_n}$ with three free parameters a_n, b_n, and c_n. The results of our fit showed that the parameters c_n are close to 1/2 for all values of n ≥ 11. Therefore we fixed the value $c_n=1/2$ and optimized the values of of a_n and b_n to get the best fits in the tail regions. Now the fit formula reads

$$\ln[P_n(U_n^2)]=a_n+b_nU_n. \tag{24}$$

The corresponding fits for the tails of the PDF's for the 11th, 15th, and 18th shells are shown in Fig. 11, lower panel. The fits are excellent for $U_n^2 > 20$ but not surprisingly they fail for smaller values of U_n^2, especially for larger values of n.

To collapse the tails together we need to choose a reference shell n_r; we show the results for $n_r=11$. Replotting $\ln[P_n(U_n^2)]-a_n+a_{11}$ as a function of $b_n^2U_n/b_{11}^2$ one collapses the tails of all the PDF's on the tail of PDF for $n_r=11$. This is shown in Fig. 12. The theoretical predictions [(16) and (20)] are

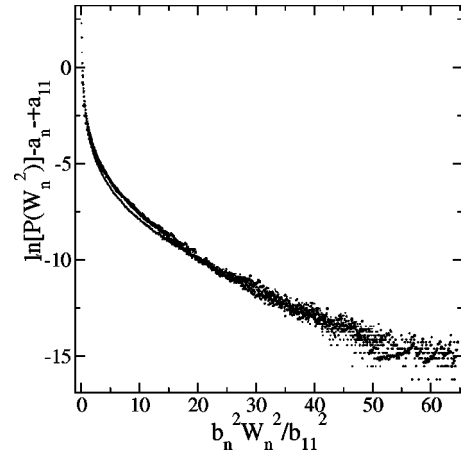$$a_n-a_{11}=(n-11)(\alpha+\beta-z)\ln\lambda, \tag{25}$$

FIG. 12. Full collapse of the PDF tails of the 11th, 15th, and 18th shells. Note that in the core region the data does not collapse.

$$2\ln(b_n/b_{11})=(n-11)\alpha\ln\lambda.$$

According to Eqs. (16) and the relation $y+z=1$ one computes $\alpha+\beta-z=2-3z+\beta$. We plot now the measured (by the best fits) values of $(b_n-b_{11})/\ln\lambda$ vs $(n-1)$. Finding best linear fits to the resulting plots we compute $\alpha=-0.25 \pm 0.03$. Noticing the independently measured values of y $=0.24\pm0.01$, $\zeta_2=0.72\pm0.01$ we see that our value of α is in excellent agreement with Eq. (16); the latter predicts α $=2y-\zeta_2\approx0.24$.

We want next to find the value of β from the first of Eqs. (25). Unfortunately the values of a_n are not computable with the same accuracy as those of b_n. The reason for this is that the fit formulas pick up the values of the intercepts of Eq. (24) with much worse precision than the slopes. Accordingly the plot $(a_n-a_{11})/\ln\lambda$ vs $(n-11)$ is much more scattered than the corresponding plot for the slopes, and we can only offer a rough estimate of the expected values of β, $0.2\leq\beta\leq0.6$.

This rough estimate is not satisfactory, and therefore we attempt now to find a sharper result for β using Eq. (23). In paper [8] we measured the values of ζ_p for $p=1,2,3,\ldots,7$. We recognize that these values of p are not large enough to determine the asymptotic slope of ζ_p. Nevertheless for a semiquantitative analysis we can use a reasonable fit formula for the ζ_p dependence, for example,

$$\zeta_p=\frac{p}{3}-\frac{\delta p(p-3)}{1+\gamma p}. \tag{26}$$

With this we find the "best" values of δ and γ that agree with the measured values of ζ_p: $\delta\approx0.092$, $\gamma\approx0.725$. With these values Eq. (26) predicts for $p\rightarrow\infty$

$$\zeta_p\approx0.56+0.21p. \tag{27}$$

According to the prediction (23) the slope of this dependence is y. The value of y found above from the intershell collapse of the separated peaks is $y=0.24\pm0.01$, being in agreement with the value of y found from the collapse of PDF tails. The value $y=0.24\pm0.01$ differs a bit from the slope in Eq. (27).

Nevertheless in light of the inaccuracy of the measured values ζ_p for large p (originating mostly from the finite extent of the inertial interval), one cannot trust the last digits in the numbers of Eq. (27). We thus consider the agreement between the estimated values of y more than acceptable.

Thus we will use the intercept in Eq. (27) to estimate β. Considering Eq. (23) the free term in Eq. (27) has to be $z - \beta$. With $z \approx 0.74$ we compute $\beta \approx 0.18$ which is at the borderline of the expected region [0.2,0.6] found above from collapsing the PDF tails. Taking then a value of $\beta \approx 0.2$ allows us to evaluate the number of peaks N_n in an n shell when there were N_{n-1} peaks in the previous one,

$$N_n / N_{n-1} = \lambda^{\beta} \approx 1.15 \quad \text{for} \quad \lambda = 2, \quad \beta = 0.2. \quad (28)$$

The conclusion is that peak splitting leads (for $\lambda = 2$ and the chosen value of a, b, c) to a 15% increase of N_n from shell to shell.

A cursory look at Fig. 6 may leave the impression that this is an underestimate. After all, from one peak in shell 15 the cascade forms four or five peaks in shell 20. A rate of increase of 15% would result in a factor of 2, not 5. But we must rememeber that we talk about peaks *of a given amplitude*, and the peak splitting results in peaks of varying amplitudes. The counting of peaks of comparable amplitudes is more subtle, and the predicted rate of 15% increase should be interpreted in the statistical sense, taking many realizations into account.

V. SELF-SIMILAR SOLUTIONS OF THE SABRA SHELL MODEL

In this section we rationalize the scale-invariant form (11) on the basis of the equations of motion of the Sabra model (2). The exponent y and the times t_n which appear in Eq. (11) are chosen according to

$$y = 1 - z, \quad t_n - t_{n-1} = A\lambda^{-zn}, \quad (29)$$

with an arbitrary positive parameter A (note that in [10] there was a salient choice of $A = 0$). These choices are not specific for the Sabra model; in Refs. [9,10] identical choices were taken the the Obukhov-Novikov (ON) and the Gledzer-Okhitani-Yamada (GOY) models. The fist relation follows from simple power counting, since the right-hand side (RHS) of the equation of motion for the nth shell is proportional to λ^n. Indeed, we saw that this scaling relation is in good agreement with our numerical observations. The second choice of Eq. (29) reflects the fact the time delay between the appearance of the peaks in consecutive n shells falls off geometrically with n; see Fig. 6 as an example. Nevertheless we want to show directly that these choices are supported by the equations of motion.

In doing so we follow Ref. [9]. Substituting Eqs. (11) and (29) in Eq. (2) we find the equation of motion of the scaling function $f(\tau)$ which is valid in the inertial interval,

$$\frac{df(\tau)}{d\tau} = \lambda^{3z-2} f^*(\lambda^z(\tau - \tau_0) + \tau_0) f(\lambda^{2z}(\tau - \tau_0) + \tau_0)$$

$$+ c\lambda^{2-3z} f(\lambda^{-z}(\tau - \tau_0) + \tau_0) f(\lambda^{-2z}(\tau - \tau_0) + \tau_0)$$

$$- (a+c) f^*(\lambda^{-z}(\tau - \tau_0) + \tau_0) f(\lambda^z(\tau - \tau_0) + \tau_0). \quad (30)$$

To get this equation we changed the time variable from t to $\tau_n \equiv \lambda^{nz}(t - t_n)$, and used the same τ_n in all the shells involved in Eq. (2), and finally denoted $\tau_n \equiv \tau$. The characteristic time τ_0 is obtained from computing the sum of all time increments $\Sigma_{m=n}^{\infty}(t_{m+1} - t_m)$, and noting that it converges to $t_0 = \lambda^{-nz} \tau_0$, where

$$t_0 = \lambda^{-nz} \tau_0, \quad \tau_0 \equiv A/(\lambda^z - 1). \quad (31)$$

The meaning of t_0 is the time needed for a pulse to propagate from the nth shell all the way to infinitely high shells. The characteristic time τ_0 allows one to convert all the arguments of the functions f involved in Eq. (30) to a universal form $[\lambda^{\delta}(\tau - \tau_0) + \tau_0]$.

It was shown in Ref. [9] that Eq. (30) can be considered as a nonlinear eigenvalue problem. It has trivial solutions $f(\tau) = 0$, but it may have nonzero solutions for particular values of z and A. For example, the nonzero solution $f(\tau) = $ const requires $z = 2/3$. Nevertheless the constant solution fails to fulfill the requirement that $\lim_{\tau \to \pm\infty} f(\tau) = 0$. We expect that a nontrivial solution that satisfied the boundary conditions will force z into the observed value which lies between 2/3 to 1. The actual calculations that demonstrate this are outside the scope of this paper. We just reiterate our numerical finding that $z \approx 0.75$ for the particular set of parameters a, b, c, and λ that were employed in this study.

VI. PREDICTING TAILS OF PDF'S FROM DATA MEASURED IN SHORT TIME HORIZONS

In this section we demonstrate that the analysis presented above can be used to predict the tails of the PDF's of large scale phenomena (relatively low values of n) using only data measured in the short time horizon. We focus on the example shown in Fig. 2, i.e., $n = 11$ with 10^7 times steps.

We first fit the PDF shown in Fig. 2, using a fit formula which is inspired by Eq. (24),

$$\ln[P_n(u_n^2)] = \tilde{a}_n + \tilde{b}_n u_n^{\tilde{c}_n}, \quad (32)$$

and found $\tilde{a}_{11} \approx 1.34$, $\tilde{b}_{11} \approx -4.64$, $\tilde{c}_{11} \approx 0.28$. The data and the best fit are shown in Fig. 13(a).

Next we want to continue the PDF of $n = 11$ into event values that are too rare in the short time horizon. To this aim we measured, in the same time window of 10^7 time steps, the tail of the PDF of the 18th shell. In doing so we use the fact that the small scale events have a much shorter turn over time, and the "short" time horizon is sufficiently long to provide a good estimate of the tail. We fitted the tail with Eq. (24) and found $a_{18} \approx -5.3$, $b_{18} \approx -0.94$. From this value and [Eq. (25)] we can predict b_{11}. We employ the value $\alpha \approx 0.24$

FIG. 14. Test of the predicted PDF for the 11th shell using data from a hundredfold longer time horizon of 10^9 time steps.
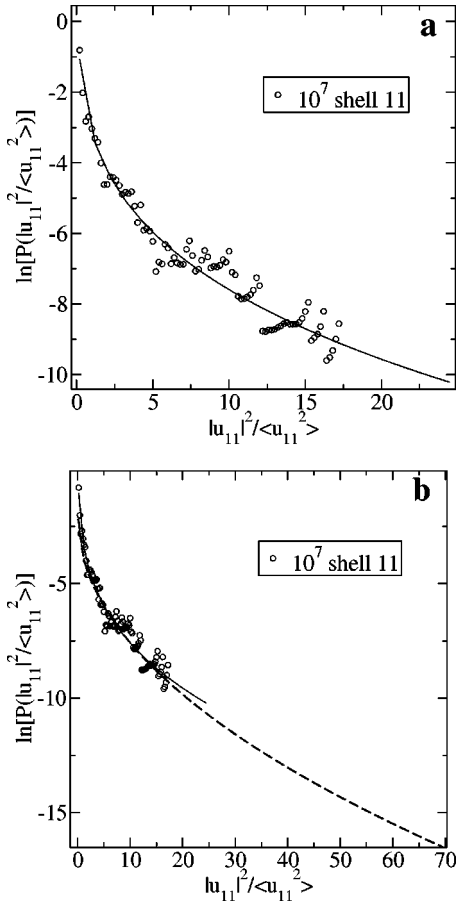
FIG. 13. (a) Data and analytic fit for the PDF of the 11th shell in a short time horizon of 10^7 time steps. Note that here we presented all the events, including four isolated events that give rise to the upswingings strings of data points with amplitudes larger than 7. (b) Same as in (a) together with the tail (dashed line) predicted from the tail of the 18th shell in the same short time horizon.

which is taken from Eq. (16) with the known value of y (from the intershell collapse) and of ζ_2. The resulting prediction is $b_{11} \approx -1.72$.

Rather than attempting to also predict a_{11} in Eq. (24) (knowing the inaccuracies of intercepts) we connected the tail with the predicted value of b_{11} to the core PDF function (32) by finding the unique point of continuity with the same first derivative. The way that the predicted tail is related to the PDF is shown in Fig. 13(b).

To test the quality of the prediction we ran now the simulation for a time horizon that is a hundred times longer (i.e., 10^9 time steps). Such a run can resolve the events that belong to the tail, and indeed the comparison is surprisingly good, as seen in Fig. 14.

VII. SUMMARY

The main aims of this paper are twofold: on the one hand we aimed at understanding the detailed dynamical scaling properties of the largest events in our system. On the other hand we wanted to employ these properties to *predict* the probability of these events even in situations in which they are very rare.
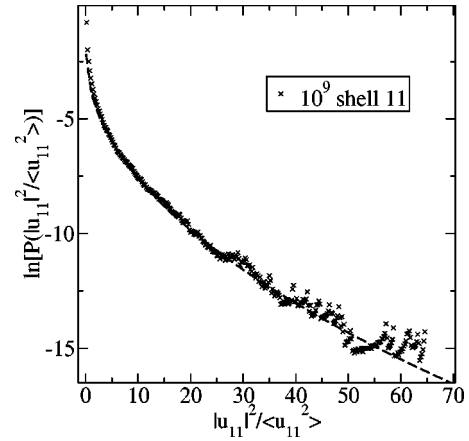
The first aim was achieved by focusing on the largest events, following their cascade down the the scales (or up the shells), and learning how to collapse them on each other by rescaling their amplitudes and their time arguments. This exercise culminated in Eq. (11) which represents the largest events $u_n(t)$ in terms of a "universal" function $f(\tau)$ where τ is a properly rescaled time difference from the peak time of the event. This dynamical scaling form is characterized by two exponents, a "static" one denoted y and a "dynamic" one denoted z. We argued theoretically for a scaling relation $z + y = 1$, and determined the values of these exponents on the basis of the analysis of isolated events in *short* time horizons.

The second aim was accomplished by developing a scaling theory for the tails of the PDF's in different shells. We have learned how to translate information from the tail of a PDF in a high shell to the tail of a PDF of a low shell. In doing so we made use of the fact that the high shells (small length scales) have much shorter characteristic times scales. Thus even short time horizons are sufficient to accumulate *reliable* statistics on the tails of the PDF's of high shells. Having a theory to translate the information to low shells in which the tails are extremely sparse (or even totally absent), we could overcome the meager statistics. We could present predicted tails that were populated only in time horizons that were a hundredfold longer than those in which the analysis was performed.

We demonstrated the existence of scaling properties of the extreme events that are in distinction from the bulk of the fluctuations that make the core of the PDF. In this sense the extreme events are outliers. We cannot, on the basis of the present work, claim that this approach has a general applicability to a large class of physical systems in which extreme events are important. We certainly made a crucial and explicit use of the scale invariance of the underlying equation of motion. This scale invariance translates here to an intimate connection between extreme events appearing on one length scale at one time to extreme events appearing on smaller length scales at later (and predictable) times (cf. Fig. 6). We are pretty confident that similar ideas can (and should) be implemented to fluid turbulence; whether or not such techniques will be applicable to broader issues like geo-

physical phenomena or financial markets is a question that we pose to the community at large.

ACKNOWLEDGMENTS

[1] D. Sornette, Phys. World **12**, 57 (1999).

[2] A. Johansen and D. Sornette, Eur. Phys. J. B **1**, 141 (1998).

[3] E. B. Gledzer, Dokl. Akad. Nauk. SSSR **200**, 1046 (1973) [Sov. Phys. Dokl. **18**, 216 (1973)].

[4] M. Yamada and K. Ohkitani, J. Phys. Soc. Jpn. **56**, 4210 (1987).

[5] M. H. Jensen, G. Paladin, and A. Vulpiani, Phys. Rev. A **43**, 798 (1991).

[6] D. Pissarenko, L. Biferale, D. Courvoisier, U. Frisch, and M. Vergassola, Phys. Fluids A **5**, 2533 (1993).

[7] R. Benzi, L. Biferale, and G. Parisi, Physica D **65**, 163 (1993).

[8] V. S. L'vov, E. Podivilov, A. Pomyalov, I. Procaccia, and D. Vandembrouq, Phys. Rev. E **58**, 1811 (1998).

[9] T. Nakano, Prog. Theor. Phys. **79**, 569 (1988).

[10] T. Dombre and Jean-Louis Gilson, Physica D **111**, 265 (1998).